Sensor and Simulation Notes

Note 152

September 1965

MEASUREMENT OF FIELDS NEAR A VERTICAL MONOPOLE*

A. L. Whitson and E. F. Vance

Stanford Research Institute

Electromagnetic Sciences Laboratory

Menlo Park, California 94025

ABSTRACT

An analysis of the field about a vertical monopole antenna driven against ground shows that at the ground the electric field contains vertical and horizontal components that are not in phase. The electric field at the surface is therefore elliptically polarized, and the properties of this field that can be accurately measured are the magnitude and direction of the axes of the ellipse and the magnitude and phase of fields along these axes. Careful measurements of the major components of the monopole field were made at frequencies between 0.5 and 510 kHz. Excellent agreement between the measured and computed fields was obtained.

The magnetic field about a radial wire in the vicinity of the monopole antenna and the current induced in the wire were also measured. The data from these measurements were found to be in agreement with a simple transmission line theory of coupling to a conductor near the surface.

*Extracted from Electromagnetic Field Distortions and Currents in and Near Buried Cables and Bunkers, AFWL-TR-65-39 of same date.

I. PURPOSE

Accurate measurement of electromagnetic fields may be used to deduce some characteristics of the source of the fields if the electromagnetic properties of the region of space containing the source and the field measurement site are known. Conversely, if the characteristics of the source of the electromagnetic fields are known, accurate measurements of the electromagnetic fields may be used to deduce some of the characteristics of the region of space about the source. In a practical experiment in which unknown source characteristics are to be determined by measuring fields about the source, it is necessary to establish, either experimentally or by construction, the characteristics of the region. One purpose of the research described in this paper was to establish the electromagnetic properties of a land area containing buried cables and other structures and subterranean geological properties by measuring the electric and magnetic fields produced at points in the area by an electric monopole antenna of known characteristics. A second purpose of this program was to determine the currents induced in the buried conductors and to establish a practical method of analysis applicable to buried conductors near the surface of the ground.

For radiated electromagnetic fields in free space, the electric and magnetic components are assumed to be orthogonal and related in magnitude by the free-space impedance. The presence of the earth,

which may not be homogeneous, can alter the field structure. To make measurements that can lead to an understanding of the cause for a particular electromagnetic field structure, all possible field parameters should be independently measured. For electromagnetic waves these parameters are the magnitude and phase of all components of the electric and magnetic fields. Thus, measurements were made over an area to determine if inhomogeneities, both known and unknown below the earth's surface, could cause the electromagnetic fields in the vicinity of a vertical radiator to differ appreciably from the fields computed assuming a homogeneous earth.

II. APPROACH

The frequency range of interest was limited to 0.5 to 510 kHz. To generate the electromagnetic field in this frequency range an easily transportable low-power switchable frequency transmitter operating at a continuous frequency of 0.5, 1, 2, 5, 10, 20.6, 62, 100, 200, 450, or 510 kHz was constructed to drive a 100-foot tower. Special narrow-band battery-powered receivers and electromagnetic field sensors were constructed to measure individual wave component magnitude and phase and component spatial orientation. [For example, the major magnetic field near the transmitter is predicted to be azimuthal and counter-clockwise about the radiating antenna. The magnetic field receiving system was designed to determine the magnitude and phase of this magnetic field and its orientation in space.] The equipment was designed so that electromagnetic fields could be mapped out to about 2 km.

Field distortions that may exist due to earth inhomogeneities are not expected to be large. Thus, very precise measurements are desirable. Design goals were signal magnitude accuracy to better than 5 percent (0.4 dB), phase accuracy to 5 degrees, and field orientation accuracy to 1 degree. These goals were essentially attained by careful equipment design and considerable testing of the entire system in an area that was free of known man-made structures. The ground conductivity in the testing area was known by measurements to a depth of 2000 feet.[1]* Simple man-made cable structures were then installed in the area to determine effects and system performance in the vicinity of such structures under relatively controlled conditions. The results of these measurements formed the basis for an analytical expression of induced cable currents.

III. EM FIELDS ABOUT A MONOPOLE ANTENNA

It is desired to determine the electric and magnetic fields produced at the air/earth interface by a short monopole antenna (length < 0.05 wavelengths) at various distances from the antenna. For this purpose, the antenna may be considered a point source of radiation with little error, since, in the range of interest, the antenna height is usually less than 10 percent of the horizontal distance to the point where the fields are to be determined. Throughout the range of fre-

---

*References are listed at the end of the paper.

quencies of interest, assuming the relative dielectric constant of the soil to be 10,

$$\frac{\sigma}{\omega\varepsilon} \approx \frac{4 \times 10^{-3}}{\frac{20\pi}{36\pi} \times 10^{-9} f} = \frac{7.2 \times 10^{6}}{f} \gg 1$$

so that for the purpose of calculating the principal components (i.e., vertical electric and azimuthal magnetic) of the fields, the ground may be treated as a good conductor. To determine the magnitude of the radial electric field, however, it is necessary to take into account the finite conductivity of the soil. Finally, because the 100-foot transmitting antenna is electrically short, the input impedance of the antenna is almost entirely capacitive reactance and the antenna input current I_0 is given by

$$I_0 \approx j\omega C_a V_a$$

where C_a is the antenna input capacitance (exclusive of the stray capacitance of the base of the antenna), and V_a is the antenna driving voltage.

In relation to the voltage applied to the antenna terminals V_a, the vertical electric field, E_θ, and the azimuthal magnetic field, H_φ, at a distance r from an electrically short monopole in phasor form,* are[2]

*Unrationalized MKS units are used throughout this paper.

$$\frac{E_\theta}{V_a} = \frac{h_e C_a}{2\pi}\left\{\left[-\frac{\omega^2\mu_0}{r} + \frac{1}{\varepsilon_0 r^3}\right] + j\frac{\omega\eta_0}{r^2}\right\} e^{-jkr}\sin\theta \qquad (1)$$

$$\frac{H_\varphi}{V_a} = \frac{h_e C_a}{2\pi}\left\{\frac{-k\omega}{r} + j\frac{\omega}{r^2}\right\} e^{-jkr}\sin\theta \qquad (2)$$

where

C_a = Antenna capacitance

h_e = Effective height of monopole in meters

ω = $2\pi f$, the signal radian frequency

μ_0 = $4\pi \times 10^{-7}$, the permeability of free space

ε_0 = $(36\pi \times 10^9)^{-1}$, the permittivity of free space

k = $\omega\sqrt{\mu_0\varepsilon_0}$, the phase constant

η_0 = $\sqrt{\mu_0/\varepsilon_0}$, the intrinsic impedance of free space

j = $\sqrt{-1}$

and r, θ, and φ are the spherical coordinates with the origin at the antenna base, and the axis of the antenna is the $\theta = 0$ line.

The radial electric field strength at the surface of a ground of finite conductivity can be computed from the surface impedance η of the earth and the azimuthal magnetic field from

$$E_r = -H_\varphi \eta$$

where

$$\eta = \frac{1 + j}{\sigma \delta} \quad ,$$

σ is the soil conductivity, and δ is the skin depth defined by

$$\delta = \frac{1}{\sqrt{\pi f \mu \sigma}} \quad .$$

The radial electric-field strength, E_r, is then

$$\frac{E_r}{V_a} = - (1 + j) \left(\frac{\pi f \mu_0}{\sigma} \right)^{\frac{1}{2}} \frac{H_\varphi}{V_a} \quad . \tag{3}$$

The effective height for the monopole has been shown by others[3,4] to be

$$h_e = \frac{h(1 - \cos kh)}{(kh)^2 \cos kh} \quad . \tag{4}$$

$$\approx \frac{h}{2} \quad (kh \ll 1)$$

The antenna input capacitance of the electrically short monopole has been shown by Schelkunoff[5] to be

$$C_a = \frac{2\pi \epsilon h}{\ln(h/a_e) - 1} \tag{5}$$

where a_e is the cylindrical antenna radius or the equivalent radius of an antenna whose cross section is noncircular. The antenna cross section used in this case is an equilateral triangle. According to Lo,[6] the radius of an equivalent cylindrical antenna is 0.4214s where s is the length of one side of the triangular cross section.

The total electric field at any point of observation around an electrically short vertical transmitting antenna is described by the two orthogonal electric field components E_θ and E_r. The received electrical signal at any distance from the transmitting antenna is the spatial vector sum of these two field components. The instantaneous values of E_θ and E_r, using phasor notation are given as follows:

$$e_\theta(t) = |E_\theta| \cos \omega t \tag{6}$$

$$e_r(t) = |E_r| \cos(\omega t + \alpha) \tag{7}$$

where α is the time phase difference of $e_r(t)$ with respect to $e_\theta(t)$. Equations (6) and (7) generally describes an electric field phasor that is elliptically polarized in the E_θ, E_r plane. The general spatial configuration for this ellipse, shown in Figure 1 is obtained by rotating the E_θ, E_r coordinates into E_1, E_2 which are the major and minor ellipse axis respectively and is simply described by[7]

$$\tan 2\tau = \frac{2\rho \cos \alpha}{1 - \rho^2} \tag{8}$$

where $\rho = |E_r|/|E_\theta|$, normally a number $< 10^{-2}$ for the case here, and τ is the space "tilt" angle of the ellipse and is the spatial angle between E_θ and the major axis, and also between E_r and the minor axis.

Examination of the electric fields defined by Eqs. (1) and (3) shows that the time angle, α, varies from $-\pi/4$ (near zone) to $-3\pi/4$

(far zone), as shown in Figure 2(a). The polarization ellipse tilt angle, τ, tilts backward for $\alpha > -\pi/2$, is vertical for $\alpha = -\pi/2$, and tilts forward for $\alpha < -\pi/2$ [shown in Figure 2(b)]. This implies that the field minimum (null) occurs at a forward angle above the horizontal in the near zone, and below the horizontal in the far zone. For negative α, which includes all situations considered here, the ellipses are always "backward" polarized--that is, they appear to be "rolling" toward the transmitter. In all cases, the ellipse must fit inside a rectangle bounded by $\pm |E_\theta|$ and $\pm |E_r|$.

The projection of e(t) on any axis at the space angle ψ shown in Figure 1 is

$$e_\psi(t) = e_\theta(t) \cos\psi + e_r(t) \sin\psi \quad . \tag{9}$$

Equation (9) can be shown to be

$$e_\psi = |E_\psi| \cos(\omega t + \zeta) \tag{10a}$$

where

$$|E_\psi| = |E_\theta| \left(\cos^2\psi + \rho \cos\alpha \sin 2\psi + \rho^2 \sin^2\psi \right)^{1/2} \tag{10b}$$

$$\zeta = \tan^{-1}\left(\frac{\rho \sin\alpha \sin\psi}{\cos\psi + \rho \cos\alpha \sin\psi} \right) \quad . \tag{10c}$$

The instantaneous field in the ψ direction, e_ψ, is always a cosinusoidal function of frequency ω and of amplitude $|E_\psi|$ and phase, ζ, both of which are determined by the axis angle, ψ, the original signals E_θ, E_r, and their time phase relation, α.

If a sensor is oriented with its maximum sensitivity in the ψ direction, the peak magnitude and phase of this sensor signal are determined by the tangent to the ellipse which is perpendicular to ψ axis (see Figure 1). Phase is determined by the point of tangency at the point (Δ) on the ellipse, and magnitude is determined by the intersection ($\blacktriangle$) of the tangent and the ψ axis. Thus, it is seen that the sensor does not always measure the magnitude and phase in the direction of the ψ axis. The sensor does measure the magnitude and phase of e(t) in the direction of the sensor when the ψ axis is aligned with either the major axis (peak field measurement), or with the minor axis (minimum or null field measurement).

The dependence of the magnitude and phase of the sensor field E_ψ is shown in pictorial form in Figure 1 as ψ is varied from π to $3\pi/2$. The circles (o) correspond to a phase point, ζ, on the ellipse for a particular position of e(t). The corresponding cross (x), with the same number, gives the sensor orientation angle ψ for observing this ζ. It is immediately apparent that the phase is changing most rapidly near the field minimum, since the (x) are more closely spaced for the relatively evenly spaced (o), and the phase is changing most slowly near the field maximum, since the (x) are more widely spaced for the relatively evenly spaced (o).

IV. CABLE CURRENT THEORY

As has been shown above, when the ground is an imperfect conductor a radial component of electric field will be produced in the ground as a result of ground currents and ground impedance. Any radially directed conductor in or near the ground will therefore have a current induced in it by the radial electric field. The manner in which the conductor is coupled to the radial electric field in the ground determines the induced current, which is of primary interest in this section.

A conductor lying in or near the ground may be visualized as a two-conductor transmission line with the ground serving as the return conductor. The line will be characterized by a series impedance per unit length and a shunt admittance per unit length, and from these a propagation factor and a characteristic impedance can be determined. In the presence of a radial electric field in the ground, the line is also driven by a distributed generator. An appropriate transmission line model for the radial conductor under the influence of a radial electric field is shown in Figure 3. The series impedance Z of the line element is due to the resistance and reactance of the conductor and the ground return, and the admittance Y of the line element is due to the capacitive susceptance between the conductor and ground and to the admittance of the ground itself. The distributed generator voltage per unit length E_r is the component of the radial electric field along the wire.

To compute the current induced in a conductor under the influence of a radial electric field, the model of the transmission line element shown in Figure 3 will be solved.[8] From the figure, the rate of change of the line voltage is

$$\frac{dV}{dx} = -IZ + E_r \tag{11}$$

and the rate of change of the line current is

$$\frac{dI}{dx} = -VY \quad . \tag{12}$$

Differentiating Eq. (12) and substituting for dV/dx in Eq. (11), we obtain the differential equation for the line currents:

$$\frac{d^2I}{dx^2} - ZYI = -YE_r \quad . \tag{13}$$

The solution of this equation is:

$$I(x) = K_1 e^{\gamma x} + K_2 e^{-\gamma x} + F(x) \tag{14}$$

where

$$F(x) = -\frac{1}{2Z_0}\left[e^{\gamma x}\int e^{-\gamma x} E_r dx - e^{-\gamma x}\int e^{\gamma x} E_r dx\right] \tag{15}$$

$$\gamma^2 = ZY$$

$$Z_0 = \sqrt{Z/Y} \quad .$$

For a particular conductor, the constants K_1 and K_2 are evaluated from

$$\frac{V(0)}{I(0)} = -Z_1 \qquad \frac{V(d)}{I(d)} = Z_2 \quad . \tag{16}$$

where Z_1 and Z_2 are the terminating impedances at the ends (x = 0) and (x = d), respectively. From Eqs. (12) and (14), the conductor-to-soil voltage is

$$V(x) = -\frac{1}{Y}\frac{dI}{dx} = -Z_0\left[K_1 e^{\gamma x} - K_2 e^{-\gamma x} + F_v(x)\right] \tag{17}$$

where

$$F_v(x) = \frac{1}{Z_0 Y}\frac{dF(x)}{dx} = \frac{1}{\gamma}\frac{dF(x)}{dx} \quad . \tag{18}$$

From Eqs. (14) and (17), therefore, the current in the conductor and the potential of the conductor relative to local undisturbed ground potential can be computed for arbitrary terminations, provided the impedance per unit length and the admittance per unit length can be determined for the conductor.

The above analysis is based on the assumption that the conductor is long compared to a skin depth in the soil and that there are no other conductors close enough to affect the ambient radial electric field in the ground (i.e., there are no other conductors within a few skin depths of the conductor under consideration). If the conductors are close enough together that mutual coupling effects become significant, the transmission line analysis becomes very complex, and other approaches to the cable current problem are desirable.[9]

The conductors of interest are buried round wires or cables which may be either insulated from the ground or in direct contact with the soil. The impedance and admittance per unit length of round wires with coaxial cylindrical return conductors are available from elementary texts on electromagnetic theory.[10] The impedance per unit length of the soil as a return path for the conductor current (see Figure 4) is:

$$Z_s = \frac{1 - j}{2\, r_1 \sigma \delta} \left\{ \frac{H_0^{(1)}\left[(1 - j)\frac{r_1}{\delta}\right]}{H_1^{(1)}\left[(1 - j)\frac{r_1}{\delta}\right]} \right\} \qquad (19)$$

where r_1 is the radius of the cylindrical hole in the soil.

The admittance per unit length of the soil is most readily obtained from the propagation factor for the soil and the impedance. Thus,

$$Y_s = \frac{\gamma_s^2}{Z_s} \qquad (20)$$

where

$$\gamma_s^2 = j\omega\mu(\sigma + j\omega\epsilon) \approx j\omega\mu\sigma \quad .$$

The series impedance per unit length of the conductor and its return is then

$$Z = Z_s + Z_w + jX_e \qquad (21)$$

where Z_w is the internal impedance of the wire and X_e is the external inductive reactance of the wire. The shunt admittance per unit length

of the conductor is

$$Y = \frac{jY_s B_e}{Y_s + jB_e} \quad . \tag{22}$$

where B_e is the capacitive susceptance of the wire insulations.

The soil impedance and admittance derived above apply strictly only to a conductor immersed in a conducting soil of infinite extent. Because the soil nearest the conductor contributes the most to the impedance and admittance, however, these impedances and admittances are approximately correct for any conductor submerged several conductor diameters below the surface of the ground.[8]

The impedance per unit length and the admittance per unit length of a buried, bare 10-guage copper wire were computed from Eqs. (21) and (22). From these, the propagation factor γ and the characteristic impedance Z_0 were computed, and it was noted that the real and imaginary parts of the propagation factor are almost equal, and that the real part is greater than 10^{-2} for almost the entire frequency range. This implies that a current in the wire is reduced by a factor of 1/3 in propagating 100 meters or less down the line (at 500 kHz the current is reduced by 1/3 in propagating only 5 meters). The current at a particular point along the line is therefore dependent only on the current and fields in the immediate vicinity and reflections are of concern only very near the end of the wire.

This situation permits a useful approximation to be made in estimating the current in bare conductors. Because the current at any point x_1 along the conductor is a function of only the local electric field $E_r(x_1)$, the differential equation for the conductor current has a solution

$$I(x) \approx \frac{E_r(x)}{Z} \tag{23}$$

at points several soil skin depths from the ends of the conductor. The impedance Z is often dominated by the impedance per unit length Z_s of the soil given by Eq. (19). For cylindrical conductors whose radii are small compared to a skin depth in the soil ($r_1/\delta \ll 1$), Eq. (19) reduces to

$$Z_s \approx \frac{1}{4\sigma\delta^2} + j\,\frac{1}{\sigma\pi\delta^2}\log\frac{\sqrt{2}\,\delta}{1.78\,r_1} \,. \tag{24}$$

Substituting this value of Z_s for Z in Eq. (23) gives

$$I(x) \approx \frac{\sigma E_r(x)\,\pi\delta^2}{\frac{\pi}{4} + j\log\frac{\sqrt{2}\,\delta}{1.78\,r_1}} \,. \tag{25}$$

Now it is observed that $\sigma E_r(x)$ is the current density in the soil and $\pi\delta^2$ is the cross-section area of a cylinder of radius δ about the wire. Thus, neglecting the weak dependence of the log term in the denominator on δ, Eq. (25) states that the current in the conductor is proportional to the current in a cylinder of soil one skin depth in radius. Note

also that the imaginary part of the impedance Z_s of Eq. (24) is similar to the inductive reactance of a coaxial transmission line, in that it contains the logarithm of the ratio of two radii, δ and r_1. Thus the treatment of the bare conductor in the soil as a two-conductor transmission line is less abstract than it initially appears.

V. MEASUREMENTS

Electric and magnetic field measurements were made near the surface of the ground using an electrically small electric dipole and an electrically small loop antenna. The electric dipole consisted of parallel plates, each having an area of 2.25 m^2, spaced 0.2 m apart. The loop antenna was a one-turn square loop with an area of 2.25 m^2 fabricated from 2-inch diameter aluminum tube. The terminal voltage of the loop and plate antennas was amplified and detected with a synchronous detector for which the reference signal was the local vertical electric field E_θ (as detected by a reference dipole.) The measured quantities were thus the in-phase and quadrature components of the loop or plate antenna signal relative to the reference dipole signal. Both antennas were mounted on gimbals so that they could be rotated about a vertical axis and a horizontal axis.

Initial measurements were made to determine the measurement system characteristics. These measurements were made over an area of earth known to be void of man-made metal conductors whose conductivity had

been measured. The E_θ and H_φ fields at a distance of 1000 ft from the vertical monopole antenna are shown in Figures 5 and 6.

As can be seen, electric field measurements and predicted fields agree to better than 5 percent. Magnetic fields agree to better than 10 percent. These percentages do not include any averaging among data points. The good agreement between theory and measurements indicates the accuracy of both.

The measured null for the plate antenna was 4 degrees wide between points 20 dB above the null. In normal operation, three readings near a null were made usually within one degree so that orientation of the total electric field was determined to better than one degree, referenced to the antenna mount which was accurate to about one degree. Electric field orientations were accurate to one degree from one antenna set-up to another set-up. For measurements using a single antenna set-up, the change in field orientation with frequency was accurate to about 1/4 degree.

The measurement of magnetic field orientation was only accurate to 2 or 3 degrees. This lesser accuracy to due to the loop null being generally 20 dB above the plate null and due to the geometry of the loop. (The diameter of one side subtends a 1.5-degree angle viewed from the center of the opposite side.)

Wire-current measurements were made on an insulated solid copper wire lying on the earth's surface along a line extending radially from

the transmitting antenna. The surface of the wire insulation was in physical contact with the surface of the earth throughout its length. except at a few short dips where the sag of the wire did not quite bring it in contact with the soil. The wire-current experiments were performed with insulated 10-guage AWG solid copper wire. The vinyl insulation on this wire is about 50 mils thick, so the outside diameter of the insulation is approximately 200 mils. In these experiments, the wire extended from a point 300 feet from the transmitter to a point 4000 feet from it and was open circuited at the ends. The wire current was measured at both ends and at many points along the wire using a clamp-on current transformer and the same synchronous detection equipment used with the loop and plate antennas.

The computed and measured magnitude of the wire currents for six test frequencies are shown in Figure 7, where the current is normalized to the transmitter voltage V_a and plotted as a function of distance from the transmitter. The phase of the wire current relative to the phase of the local vertical electric field E_θ is shown in Figure 8.

As is apparent in Figure 7, the form of the computed current magnitudes is remarkably similar to the form of the measured currents, particularly at 200 kHz and lower frequencies. The computed current magnitudes are slightly lower than the measured currents at frequencies of 62 kHz and higher and are considerably lower at 2 and 10 kHz; however, this is

attributable to the fact that below 10 kHz, the skin depth in the soil is greater than 300 ft, so that the electric field in the soil is greater than that given by Eq. (3).

The computed phase of Figure 8 is also in good agreement with the measured phase except at 510 kHz. At 510 kHz, the measured phase relative to the local vertical electric field decreased rapidly between 1000 and 2000 ft, but the computed phase increased in this interval. Thus, as the end of the wire at 4000 ft is approached, the measured phase is about 360 degrees less (more negative) than the computed phase. The apparant reason for this peculiar behavior of the phase at 510 kHz is that the attenuation used in computing the current was higher than the actual attenuation. Thus, in the theoretical case, the current induced in the first few hundred feet of wire was so greatly attenuated in propagating a few hundred feet that it was no longer of sufficient magnitude to be the dominant factor in determining the phase. In the experimental case, however, the attenuation at 510 kHz was apparently much lower, and the large current induced in the first few hundred feet of the wire was still large enough after propagating to 2000 ft and beyond, to be the dominant current in determining the phase of the current.

Field measurements were made to determine the effects of wire currents on the magnetic field in the vicinity of the wire. These measurements were made at 1750 ft from the transmitter above the 10 guage

wire and at 10, 20, 40, and 80 ft counter-clockwise from the wire. The vertical component of the magnetic field, H_θ, is shown in Figure 9 for the various distances from the wire. H_θ in a free-space region was measured to be in excess of 40 dB below the H_φ field component shown in Figure 9.

The current in the wire creates a magnetic field that adds to the incident H_φ field to cause an elliptic polarization of the resultant H vector more general than that shown for the E vector since the two H fields are no longer orthagonal in space. The resulting field polarization is shown in Figure 10 as tilt of the H_φ field. Both Figures 9 and 10 show the influence of wire currents on the magnetic field to at least 80 ft from the wire.

VI. CONCLUSIONS

It has been shown that electromagnetic fields in the vicinity of the ground contain more than one electric field component and generally add to form an elliptically polarized wave. Measurements on an elliptically polarized field are generally restricted to the magnitude and phase of the major elliptical component and to the spatial orientation of the major axis of the total field. Measurement of the minor field component is only possible when the two field components are within about one order of magnitude of each other.

A simplified theory of the current induced in horizontal conductors near the surface of the earth has also been developed for frequencies such that the soil behaves as a good conductor. This theory has been substantiated by an experiment in which the current in a wire on the surface of the ground was measured and the properties of the soil and the electromagnetic field about the wire were measured. The measured fields and currents are in general agreement with those predicted for the antenna and soil properties involved.

REFERENCES

1. J. R. Scott, :Electrical resistivity of earth sediments near dipole antenna site...," Technical Letters: Special Projects-10, United States Department of the Interior, Geological Survey, Denver, Colorado, January 1964.

2. S. Ramo and J. R. Whinnery, Fields and Waves in Modern Radio, 2nd ed., New York: John Wiley & Sons, pp. 497-98, 1953.

3. S. Schelkunoff and H. T. Friis, Antennas: Theory and Practice, Sec. 10.5, New York: John Wiley & Sons, 1952.

4. J. D. Kraus, Antennas, New York: McGraw-Hill, p. 230, 1950.

5. S. Schelkunoff, op, cit., Sec. 10.3, Eq. (11).

6. Y. T. Lo, "A note on the cylindrical antenna of noncircular cross section", J. Appl. Phys., vol. 24, part 2, no. 10, pp. 1338-39, 1953.

7. J. D. Kraus, op. cit., pp. 464-484

8. E. D. Sunde, Earth Conduction Effects in Transmission Systems, New York: D. Van Nostrand Co., p. 16, 1949.

9. J. R. Wait, Proc. IRE (Letters) vol. 46, August 1958, pp. 1539-41.

10. S. Ramo and J. R. Whinnery, op. cit., p. 253

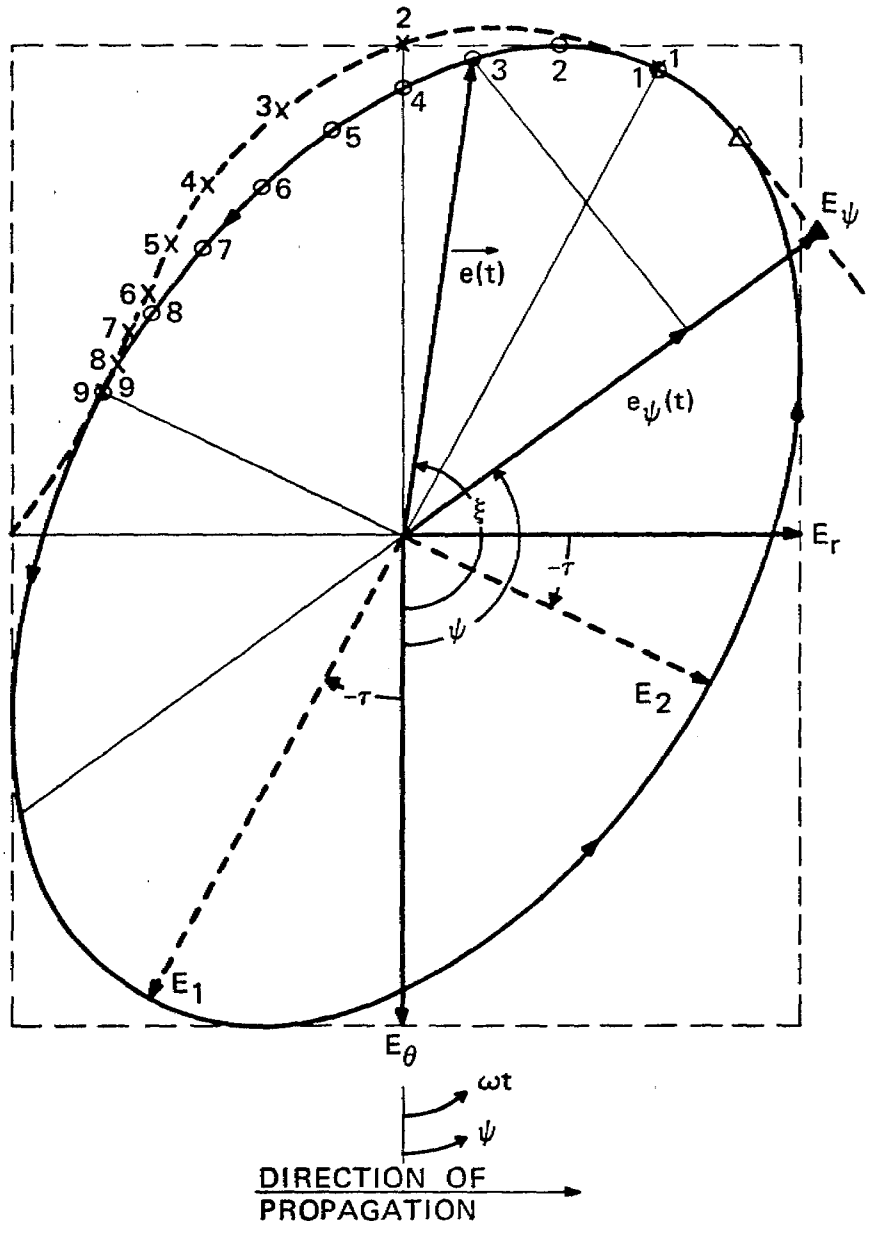

Figure 1 Polarization Ellipse for E Field ($\alpha = -3\pi/4$)

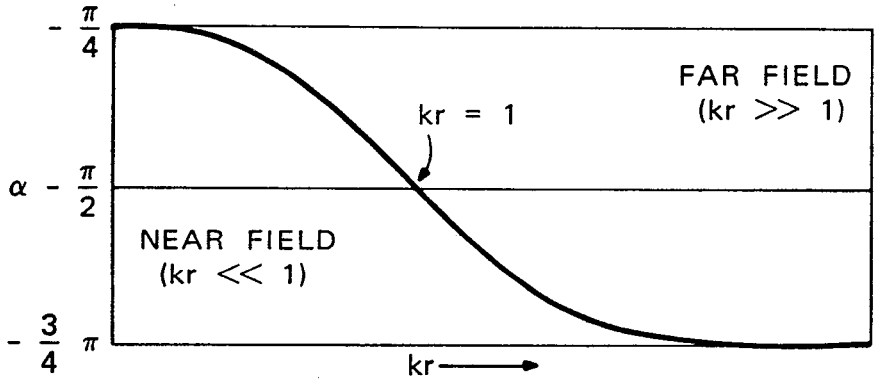

(a) SKETCH OF α FROM NEAR FIELD TO FAR FIELD AS A FUNCTION OF (kr)

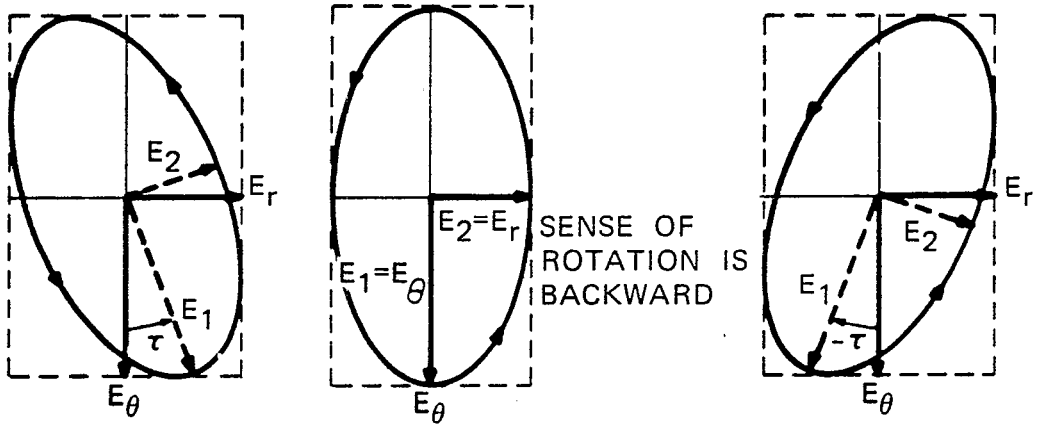

(b) SKETCH OF POLARIZATION ELLIPSES FOR α

Figure 2 Polarization Ellipse as Function of kr

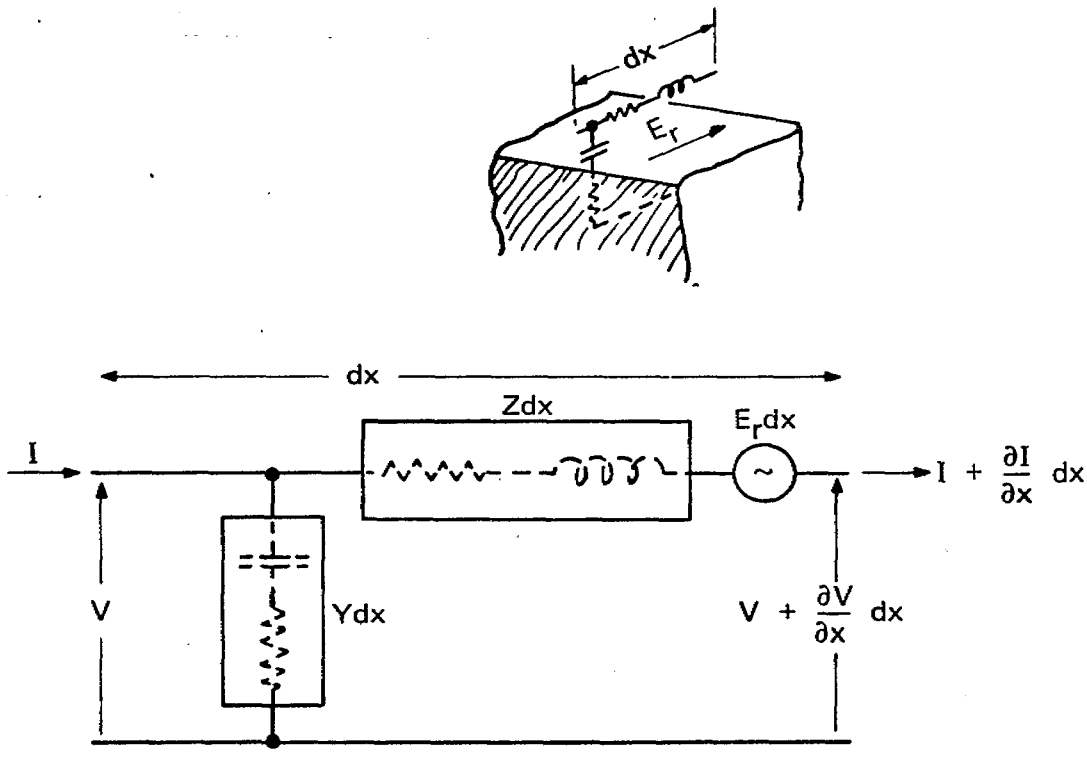

Figure 3 Transmission Line Model of Radial Conductor

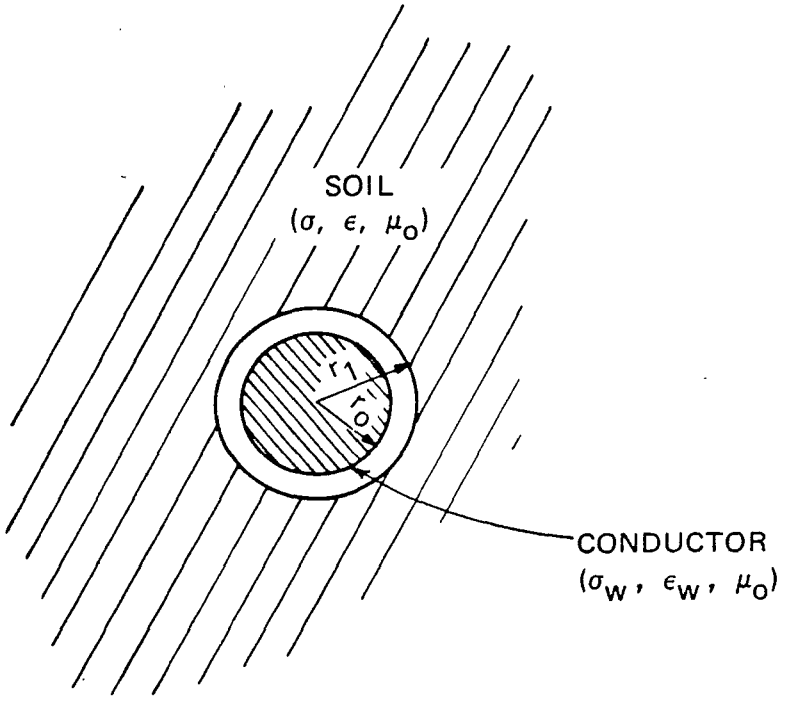

Figure 4 Round Conductor Immersed in Conducting Soil

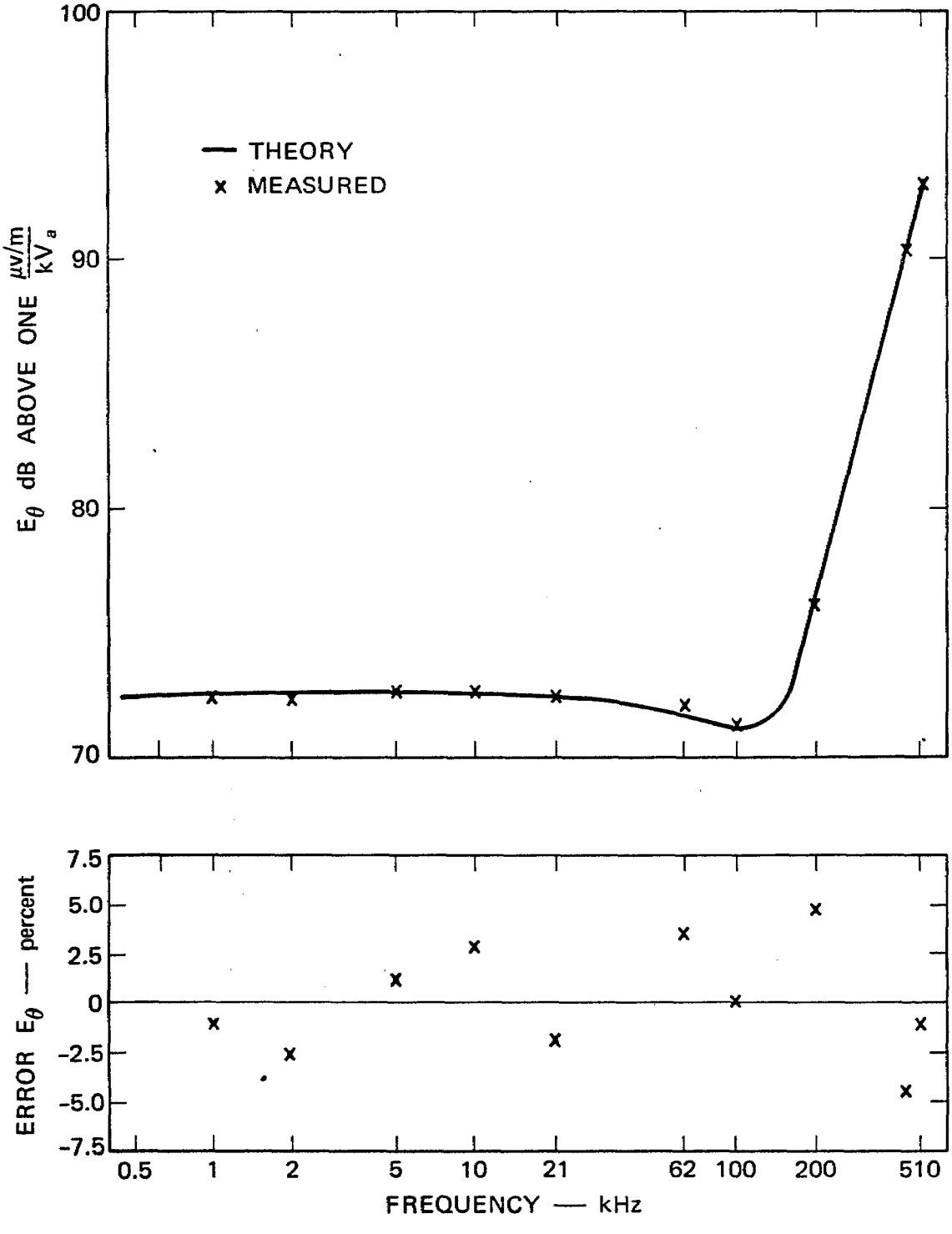

Figure 5 Measured E_θ Field at 1000 ft

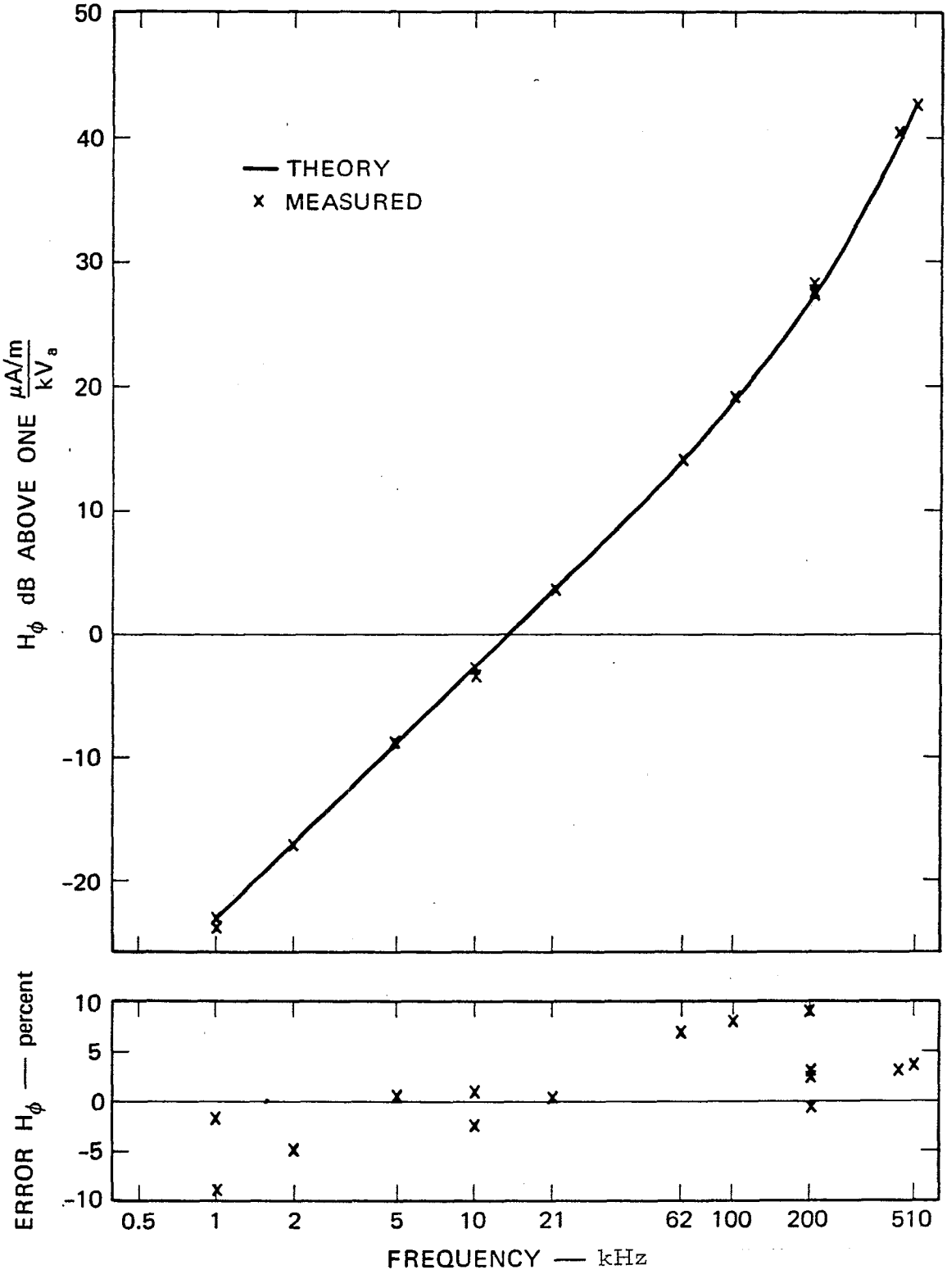

Figure 6 Measured H_φ Field at 1000 ft

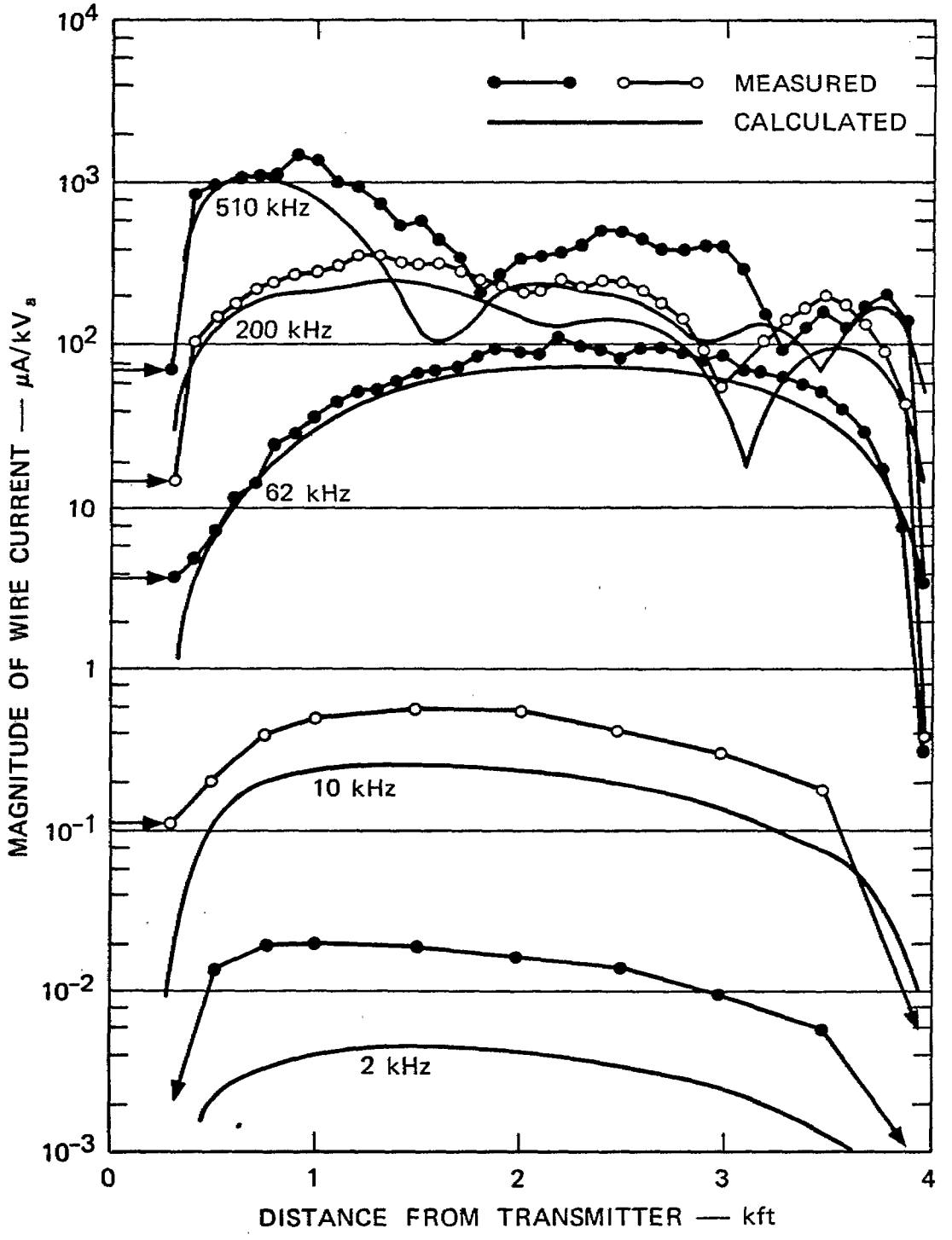

Figure 7 Computed Magnitude of Current Induced in 10-Gauge Insulated Wire

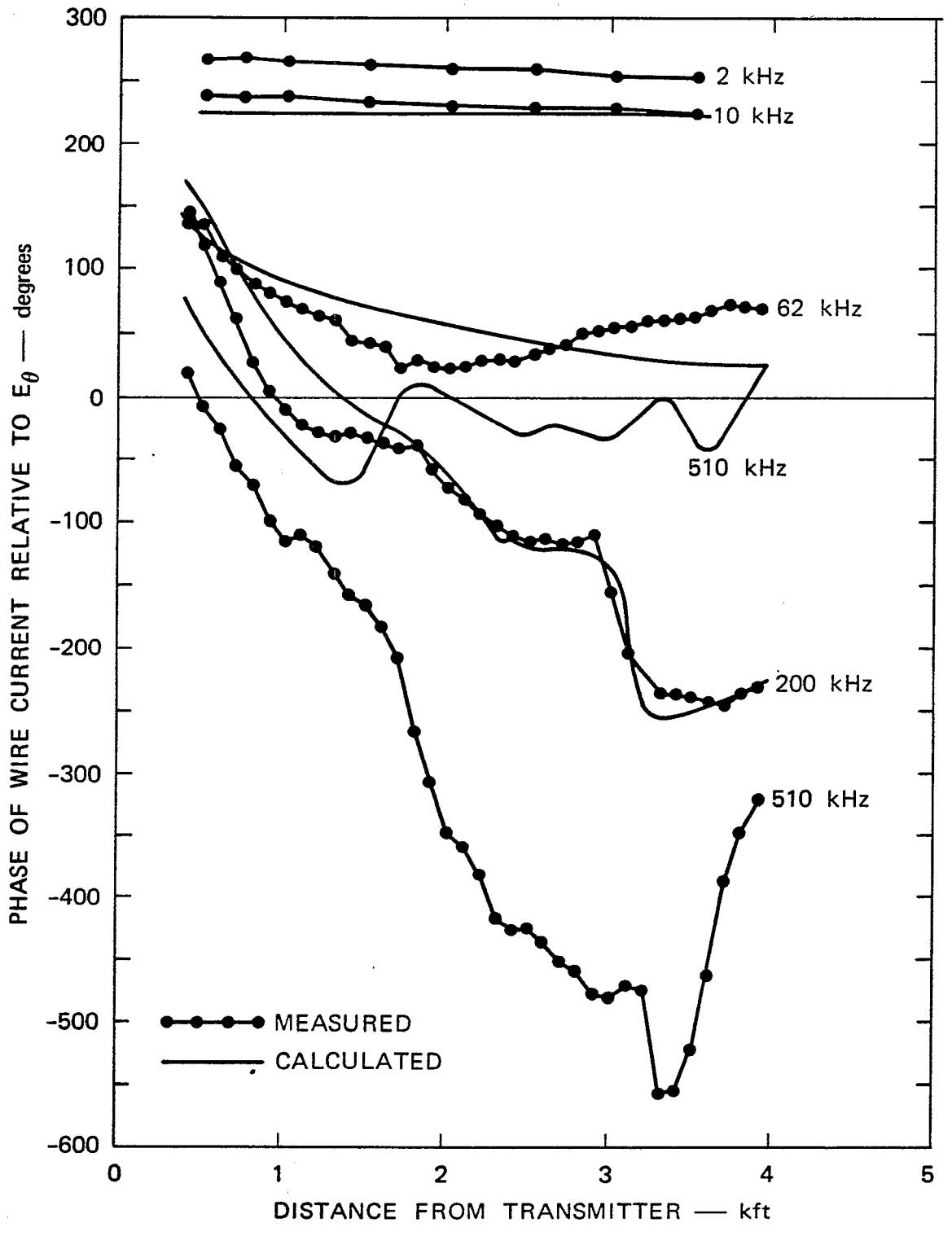

Figure 8 Measured Phase of Current Induced in 10-Gauge Insulated Wire

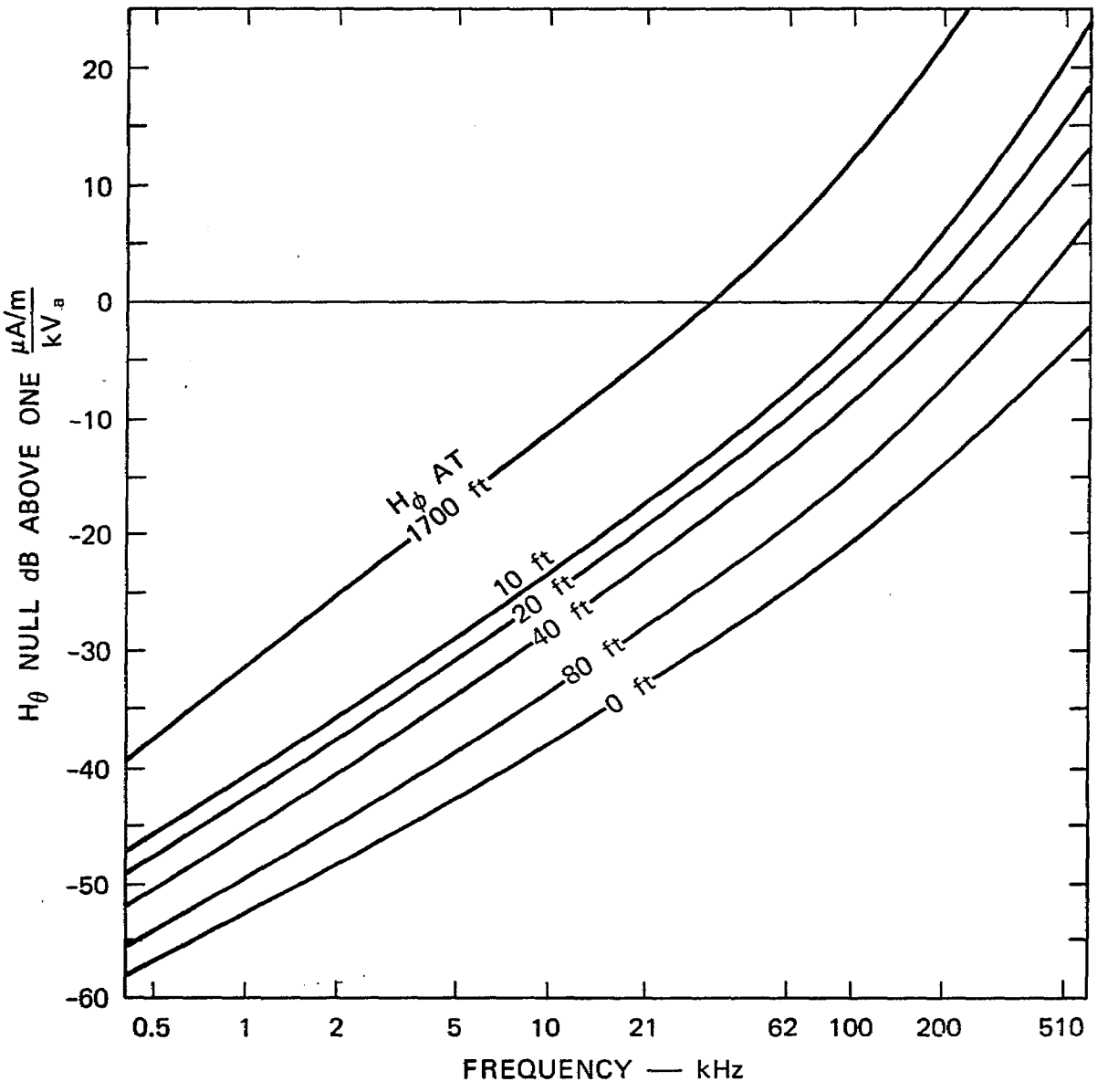

Figure 9 H_θ Magnitude Near 10-Gauge Insulated Wire

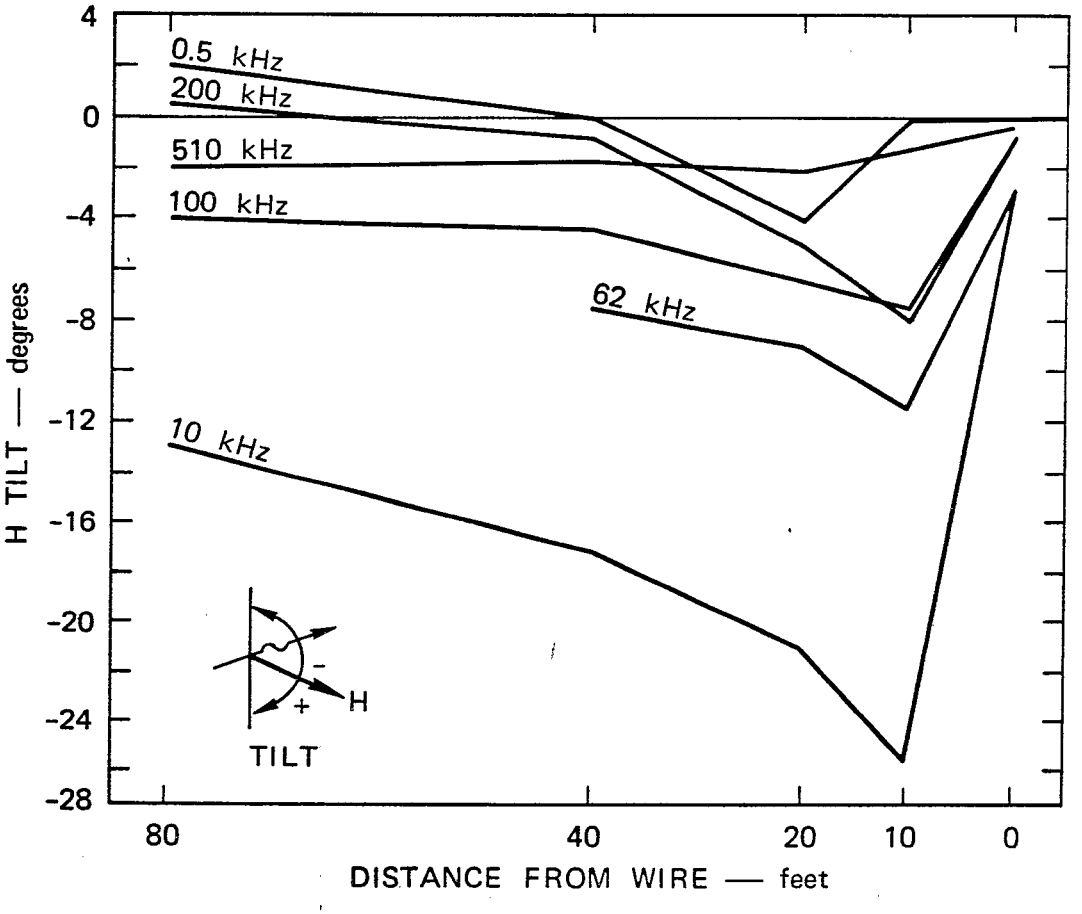

Figure 10 H Tilt Near 10-Gauge Insulated Wire